Published in final edited form as:
J Autoimmun. 2007 ; 29(2-3): 174–186. doi:10.1016/j.jaut.2007.07.005.

Species-specific immune responses generated by histidyl-tRNA synthetase immunization are associated with muscle and lung inflammation

Yasuhiro Katsumata[a], **William M. Ridgway**[a], **Timothy Oriss**[b], **Xinyan Gu**[a], **David Chin**[a], **Yuehong Wu**[a], **Noreen Fertig**[a], **Tim Oury**[c], **Daniel Vandersteen**[d], **Paula Clemens**[e], **Carlos J. Camacho**[f], **Andrew Weinberg**[g], and **Dana P. Ascherman**[a,*]

a*Department of Medicine, Division of Rheumatology and Immunology, University of Pittsburgh School of Medicine, Pittsburgh, PA 15261, USA*

b*Department of Medicine, Division of Pulmonary, Allergy, and Critical Care Medicine, University of Pittsburgh School of Medicine, Pittsburgh, PA 15213, USA*

c*Department of Pathology, University of Pittsburgh School of Medicine, Pittsburgh, PA 15261, USA*

d*Department of Pathology, St. Mary's/Duluth Clinic Health System, Duluth, MN 55805, USA*

e*Department of Neurology, University of Pittsburgh School of Medicine, Pittsburgh, PA 15261, USA*

f*Department of Computational Biology, University of Pittsburgh, Pittsburgh, PA 15261, USA*

g*Department of Basic Immunology, Earle A. Chiles Research Institute, Providence Portland Medical Center, Portland, OR 97213, USA*

Abstract

Evidence implicating histidyl-tRNA synthetase (Jo-1) in the pathogenesis of the anti-synthetase syndrome includes established genetic associations linking the reproducible phenotype of muscle inflammation and interstitial lung disease with autoantibodies recognizing Jo-1. To better address the role of Jo-1-directed B and T cell responses in the context of different genetic backgrounds, we employed Jo-1 protein immunization of C57BL/6 and NOD congenic mice. Detailed analysis of early antibody responses following inoculation with human or murine Jo-1 demonstrates remarkable species-specifity, with limited cross recognition of Jo-1 from the opposite species. Complementing these results, immunization with purified peptides derived from murine Jo-1 generates B and T cells targeting species-specific epitopes contained within the amino terminal 120 amino acids of murine Jo-1. The eventual spreading of B cell epitopes that uniformly occurs 8 weeks post immunization with murine Jo-1 provides additional evidence of an immune response mediated by autoreactive, Jo-1-specific T cells. Corresponding to this self-reactivity, mice immunized with *murine* Jo-1 develop a striking combination of muscle and lung inflammation that replicates features of the human anti-synthetase syndrome.

Keywords

Autoantibodies; Autoantigens; Inflammatory myopathy; Lung inflammation; Animal models

*Corresponding author. Department of Medicine, Division of Rheumatology and Immunology, University of Pittsburgh School of Medicine, BST S707, 3500 Terrace Street, Pittsburgh, PA 15261, USA. Tel.: +1 412 383 8734; fax: +1 412 383 8864. *E-mail address:* ascher@pitt.edu (D.P. Ascherman)..

1. Introduction

Polymyositis (PM) and dermatomyositis (DM) represent autoimmune diseases in which muscle is inappropriately targeted for immune-mediated destruction. Both of these inflammatory myopathies can produce systemic complications that include vasculopathy (Raynaud's phenomenon), arthritis, dysphagia, cardiac dysfunction, and interstitial lung disease [1]. Yet, this clinical overlap contrasts with histologic findings that reflect potential differences in the immunopathogenesis of these two entities. While DM is characterized by perivascular B cells, CD4 + T cells, and membrane attack complex formation (terminal complement components C5-C9), the immunohistologic hallmarks of PM include endomysial T cells (CD4+ and CD8+) and the absence of complement deposition [2-4]. Thus, DM appears to result from immune complex-triggered vascular/perivascular inflammation, whereas PM stems from T cell-mediated cytolysis/dysfunction of muscle cells [5].

Despite the wealth of data supporting a primary role for T cells in the pathogenesis of PM, the antigenic trigger(s) for T cell-mediated autoimmunity in this disorder remain undefined. An important clue, however, lies in the clinical specificity of patient subsets defined by autoantibodies directed against antigens such as histidyl-tRNA synthetase (Jo-1) [6]. Antibodies recognizing a number of different tRNA synthetases, of which anti-Jo-1 are the most common, serve as the serologic hallmark of the anti-synthetase syndrome that consists of myositis, interstitial lung disease, arthritis, and fever [6]. Of note, the lack of serologic overlap between these subsets indicates that antibody formation reflects a specific, antigen-driven process rather than a bystander response to muscle injury (in which case multiple antibody specificities would be expected to co-exist).

Although previous work including histomorphologic studies does not support a direct role for anti-Jo-1 antibodies in the pathogenesis of PM, several additional pieces of evidence from extensive analysis of the B cell response in this disease implicate Jo-1 as a pathogenic autoantigen. First, antibody titers against Jo-1 correlate with disease activity in these patients [7-9]. Second, epitope mapping studies have demonstrated an increasingly complex, polyclonal anti-Jo-1 antibody response that recognizes several different portions of Jo-1, disfavoring a simple molecular mimicry hypothesis in which cross-reactive antibodies directed against a different target molecule should only bind a single epitope of Jo-1 [8,10-12]. Third, and most significantly, serial binding studies demonstrate affinity maturation of the Jo-1 antibody response over time [10]. Because antigen-specific B cell responses are ultimately T cell driven [13], this collective data strongly suggests that Jo-1 serves as a triggering antigen for CD4 + T cells that provide help for B cells as well as cytolytic T cells directed against myocytes expressing Jo-1.

Consistent with this hypothesis, we have previously demonstrated Jo-1-specific T cells in the peripheral blood of Jo-1 antibody-positive patients [14]. However, because T cells targeting Jo-1 can also be found in individuals without disease [14], a direct link between such T cells and myocytotoxicity is currently lacking. Establishing appropriate *in vitro* and *in vivo* models to analyze Jo-1-specific T cell clones is therefore necessary to determine whether antibodies targeting Jo-1 merely represent markers of disease or reflect *pathogenic*, *antigen-specific* T cell responses. Unfortunately, most of the existing animal models of myositis have provided little more than general insight concerning candidate autoantigens, under-scoring the need for newer systems that explore the basis of the clonal/oligoclonal T cell expansion found in diseased muscle of human PM patients [15,16].

While various models of other autoimmune diseases show that TCR (T cell receptor) repertoire is a key component in the breakdown of tolerance to self-antigen, disease expression ultimately depends on factors that influence T cell effector *function*. Genetic studies in congenic strains

of NOD mice provide additional insight concerning the relative contributions of T cell structure (i.e., TCR repertoire) and function to tolerance breakdown in autoimmune diabetes. Pertinent to model development for Jo-1-induced myositis, this and other work suggests that both MHC and non-MHC loci of different genetic strains are critical variables contributing to any potential disease phenotype [17]. NOD congenic variants therefore represent an ideal system for the analysis of Jo-1 immunization protocols and the impact of genetic background on disease expression, particularly given the underlying "defects" in tolerance as well as generalized autoimmune diathesis linked to the parental NOD genotype [18-23]. In the context of these different genetic backgrounds, the following studies demonstrate that B cell and, by extension, T cell responses to Jo-1 immunization are remarkably species-specific despite >95% homology between the murine and human versions of this protein. Based on the specificity of this response, we have used *murine* Jo-1 to generate autoreactive B and T cells against native Jo-1 that ultimately produce muscle and lung inflammation paralleling the human anti-synthetase syndrome.

2. Materials and methods

2.1. Antigen preparation

Recombinant fragments as well as full length versions of both human and murine histidyl-tRNA synthetase (Jo-1) were generated as maltose binding protein (MBP) fusion proteins following subcloning of appropriate sequences into the bacterial expression vector pMALc2 (New England Biolabs, Ipswich, MA). *In situ* mutagenesis (Stratagene, La Jolla, CA) with insertion of a stop codon after base pair 453 yielded constructs encoding 151 amino acid fragments of both human (HA) and murine (MA) Jo-1. While the human sequences were derived from a cDNA library of a healthy control subject, mouse Jo-1 cDNA was obtained via RT-PCR amplification of C57BL/6 myocyte RNA (courtesy of C.C. Liu). Expressed proteins were purified with amylose resin per the manufacturer's protocol (New England Biolabs, Ipswich, MA), filter sterilized, and then subjected to additional column purification for endotoxin removal (Profos AG, Regensburg, Germany) prior to use in proliferation assays. As previously described [14], full length versions of Jo-1 were cleaved with Factor Xa (New England Biolabs, Ipswich, MA) to release the MBP moiety and further purified using ion exchange chromatography.

Overlapping peptides (18-20 mers) comprising the amino terminal 120 amino acids of murine Jo-1 were synthesized and HPLC purified by the University of Pittsburgh Molecular Medicine Institute using Fmoc chemistry.

2.2. Antibodies and reagents

OX86 (provided by Andrew Weinberg) is a purified rat IgG1 OX40 agonist generated from a commercially available hybridoma as previously described [24]. Antibodies for cell surface staining included rat anti-mouse CD19 (Caltag Laboratories, Burlingame, CA) and rat anti-mouse CD4 (BD Pharmingen, San Diego, CA).

2.3. Mouse immunization

Eight to ten week old mice of the following strains were used in immunization protocols approved by the University of Pittsburgh IACUC: C57BL/6 (B6), B6.G7 (NOD I-A^{g7} MHC Class II locus crossed onto the C57BL/6 background), NOD, and NOD.*Idd3/5* (C57BL/6 Insulin dependent diabetes *Idd3/5* non-MHC loci transgressed onto the NOD background). Two hundred micrograms of the indicated antigens were emulsified with CFA in a 1:1 ratio and then injected at the base of the tail in a total volume of 200 μl. Where indicated, 100 μg (in 100 μl PBS) of OX86 was administered intraperitoneally on days 0 and 2. At designated time points (10-14 days for short term immunization, 8-16 weeks for long term immunization),

animals were sacrificed for harvesting of blood, spleen, inguinal/peri-aortic lymph nodes, quadriceps/hamstring muscles, lungs, liver, and kidneys.

2.4. Immunoprecipitation

Twenty microliters of serum samples were combined with 2 mg Protein A/G Plus agarose beads (Santa Cruz Biotechnology, Santa Cruz, CA) and bound overnight at 4 °C. After 3 washes with immunoprecipitation (IP) buffer, sepharose-bound antibodies were incubated at 4 °C for 2 h with ^{35}S methionine-labeled extract derived from approximately 1×10^6 rapidly dividing K562 cells or the mouse hybridoma partner line BW5147. Sepharose bead complexes were subsequently washed 3 times with IP buffer, suspended in 2× Laemmli sample buffer, and electrophoresed at 200 V on a standard size 10% gel. Following enhancement with 0.5 M sodium salicylate, gels were dried and subjected to autoradiography for 24-72 h. Use of a Jo-1-reactive human control serum permitted identification of the appropriate ~50 kDa band representing either human or murine Jo-1.

2.5. ELISA

IgG anti-MJo-1, HJo-1, and MBP antibody levels in the sera of mice immunized with different versions of full length Jo-1 or fragments thereof were measured using standard solidphase ELISA according to the following protocol. Ninety six-well microtiter plates (Nunc, Rochester, NY) were coated with gel purified MJo-1 (0.1 μg/ml), HJo-1 (0.1 μg/ml), or MBP (0.1 μg/ml) in carbonate buffer (50 mM NaHCO3/Na2CO3, pH 9.6) and incubated overnight at 4 °C. Plates were then washed four times with PBS containing 0.05% Tween-20. After blocking wells with PBS containing 1% BSA, appropriately diluted serum samples (1:5000) from immunized mice were added for 2 h. Following a 60 min incubation with horseradish peroxidase-conjugated goat anti-mouse IgG (0.04 μg/ml, Santa Cruz Biotechnology, Santa Cruz, CA), enzymatic reaction was visualized using 3,3,5,5-Tetramethylbenzidine (TMB) (Sigma-Aldrich, St. Louis, MO) and subsequently terminated with 1 N H_2SO_4. Color development was measured at 450 nm by a Wallac 1420 multilabel counter (PerkinElmer, Wellesley, MA), and values were plotted as OD_{450} substrate antigen - OD_{450} no antigen. For assessment of IgG antibody titers in mice immunized with Jo-1 peptide/CFA emulsions, diluted serum (1:500) was applied to wells coated with MA/MBP (2 μg/ml), HA/MBP (2 μg/ml), or MBP (2 μg/ml) according to the same protocol. All assays were performed in triplicate wells.

2.6. CFSE proliferation and flow cytometry

Spleens from immunized or control animals were mechanically disrupted and filtered through 70 micron mesh to generate whole splenocyte populations. After RBC lysis using a standardized buffer (Biolegend, San Diego, CA), cells were washed in PBS and then labeled with 0.4 μM CFSE (Molecular Probes, Eugene, OR) per the manufacturer's protocol. In 48 well plates, 6×10^5 CFSE-labeled splenocytes/well were then combined with designated antigens in 400 μl of RPMI 1640 containing 10% FCS, sodium pyruvate, non-essential amino acids, 5×10^{-5} M 2-ME, and penicillin/streptomycin. After 96 h, cells were stained with Allophycocyanin (APC)-conjugated anti-CD19 or anti-CD4 antibodies and fixed in 2% paraformaldehyde prior to flow cytometric assessment.

2.7. Histology

Harvested organs were fixed in 10% formalin prior to paraffin embedding, sectioning, and staining with hematoxylin/eosin by the University of Pittsburgh's Department of Transplant Immunology core histopathology laboratory.

Following these staining procedures, a blinded pathologist independently scored/confirmed the severity of inflammation in lung tissue. This rating was based on the relative area of

lymphocytic infiltration in multiple fields viewed under high power magnification and consisted of a 0-4 scale: 0 = no inflammation, 1 = minimal, 2 = moderate, 3 = moderate/severe, 4 = severe. For muscle tissue (also reviewed in blinded fashion), a non-quantitative scoring system based on the presence or absence of lymphocytic infiltrates was employed.

2.8. Statistics

Severity scores for lung inflammation were compared using the Mann-Whitney *U*-test. Differences in frequency of muscle inflammation (recorded as present or absent) were assessed with Fisher's exact test.

3. Results

3.1. Cloning and expression of Jo-1

Because the amino terminal portion of human histidyltRNA synthetase (Jo-1) contains immunodominant B and T cell epitopes [11,12,14], we generated recombinant fusion proteins encompassing the murine and human equivalents of this region (MA/MBP and HA/MBP, respectively) for use in subsequent immunization trials. cDNA encoding full length versions or fragments of both human and murine Jo-1 were subcloned into the bacterial expression vector pMALc2 using a combination of PCR amplification and *in situ* mutagenesis (Fig. 1A). The source of murine Jo-1 cDNA was C57BL/6 myocyte RNA, and amino acid sequence analysis revealed overlap with two previously published sequences. Of note, the sequence of the amino terminal fragment A (MA) is identical to both published sequences and differs from the human version (HA) by 10 amino acids, yielding 93% homology (Fig. 1B). The full length sequences of human and murine Jo-1 vary by 24 amino acids (95% homology), indicating that a disproportionate number of the amino acid discrepancies between the human and murine versions of this protein are located in the amino terminal 150 amino acids.

3.2. Antibody response to short term immunization

To identify the optimal protein immunization protocol promoting recognition of native/murine Jo-1, C57BL/6 (B6), NOD, and congenic strains thereof were inoculated with various Jo-1-based proteins emulsified in CFA. Review of the immunoprecipitation data in Fig. 2A indicates that immunization of different strains with full length human Jo-1 (HJo-1) or the amino terminal fragment HA fusion protein (HA/MBP) generates a robust initial antibody response 10 days post immunization that recognizes Jo-1 extracted from a human cell line (K562); interestingly, this antibody response is fairly specific for human Jo-1, showing minimal cross reactivity to mouse Jo-1 derived from a murine hybridoma partner (compare lanes 2, 3, 10, and 11 in the two panel of Fig. 2A). Conversely, animals immunized with murine versions of Jo-1 develop antibodies highly specific for murine Jo-1 with little detectable reactivity against human Jo-1 (lanes 4, 5, 12, and 13 in the two panels of Fig. 2A). When both human and murine Jo-1 are combined in protein/CFA emulsifications, the antibody response to either version of these proteins appears attenuated. ELISA results using gel purified HJo-1 or MJo-1 as substrate antigens effectively quantify the early antibody response (Fig. 2B) and again show minimal cross reactivity. Of note, the species-specific antibodies generated by immunization with HA/MBP and MA/MBP indicate that dominant B cell epitope(s) must reside in unique, rather than shared, structural portions of these antigens.

3.3. Peptide immunization

Although this class-switched antibody formation is indicative of an underlying antigen-specific T cell response, we sought to more conclusively demonstrate the existence of autoreactive T cells recognizing native Jo-1 (without the confounding influence of MBP present in fusion proteins) through immunization of NOD.*Idd3/5* and B6.G7 mice with different pools of

overlapping synthetic peptides spanning the amino-terminal portion of murine Jo-1 (Fig. 3A). Fig. 3B reveals that immunization with peptide pool 1 (P1, representing amino acids 1-58) generates reactive T cells that preferentially respond to the peptides contained within this pool, whereas immunization with peptide pool 2 (P2, covering amino acids 51-120) triggers a somewhat weaker response with the opposite specificity (P2 > P1-stimulated proliferation). More refined mapping of peptide-induced proliferation in P1-immunized mice reveals T cell recognition of several epitopes encompassed by individual peptides 1-4 (data not shown), each of which possesses amino acid substitutions differentiating them from the human sequences spanning the same region (amino acids 1-48).

When tested by ELISA 14e24 days post immunization, serum samples from P1-immunized animals show striking IgG antibody recognition of MA/MBP, but not HA/MBP (Fig. 3C). Because these antibodies have undergone isotype switching, their development confirms peptide-specific T cell responses shown in the CFSE proliferation experiments of Fig. 3B. Interestingly, immunization with P2 also triggers significant, preferential antibody recognition of MA/MBP in some B6.G7 mice—despite 98% sequence homology between MA and HA in this region spanning amino acids 51-120. Corroborating these results, immunization of NOD.*Idd3/5* mice with individual peptides reveals that sequences in the regions encompassed by P1 and P2 can trigger antibody formation specific for MA/MBP, but not HA/MBP (Fig. 3D). What is most striking, however, is that peptides with 100% sequence homology between murine and human Jo-1 stimulate antibodies that selectively recognize murine Jo-1 (amino acids 51-68, 71-88, 81-98; Fig. 3D, open figures). Analysis of peptide recognition profiles in sera obtained 14 days post immunization with MA/MBP confirms these observations, as several shared linear sequences represent dominant or co-dominant targets of antibodies that are highly specific for murine Jo-1 (data not shown). Collectively, these findings suggest that the basis of species-specific B cell responses following Jo-1 *protein* immunization relates to *structural* as well as sequence variation between murine and human Jo-1 (ultimately impacting exposure/availability of identical linear epitopes).

3.4. Long term B cell responses

Given the combined evidence that immunization with peptides or protein fragments comprising murine Jo-1 generates specific B and T cell responses against the native/self version of this protein, we established longer term immunization protocols for evaluation of tissue phenotype in B6.G7 and NOD.*Idd3/5* mice (which share the NOD I-A^{g7} MHC II locus but have different non-MHC backgrounds). Ultimately, this strain selection/comparison permitted assessment of potential non-MHC genetic contributions without the confounding influence of autoimmune diabetes that occurs in parental NOD mice.

Paralleling the B cell responses noted 10 days following immunization with MA/MBP or HA/MBP, immunoprecipitation studies of serum samples obtained 8 weeks after immunization reveal a breakdown of B cell tolerance to murine Jo-1 primarily in MA/MBP-immunized cohorts (Fig. 4A). Because ELISA results show that anti-Jo-1 antibodies include IgG isotypes indicative of class switching and T cell-dependent B cell responses, these results likely reflect a breakdown in T cell tolerance to self/murine Jo-1 (see below).

Further evidence of an evolving immune response to Jo-1 in MA/MBP-immunized mice is the antibody cross recognition of human Jo-1 occurring after 8 weeks that is not observed in animals sacrificed at very early time points (compare Figs. 2A (upper panel) and 4A (lower panel), 10 days versus 8 weeks). Interestingly, the cross recognition of human Jo-1 in MA/MBP-immunized mice that occurs by 8 weeks is most evident when assessed by immunoprecipitation (versus ELISA), likely reflecting differences between binding of conformational epitopes in native protein (immunoprecipitation) and linear epitopes of partially denatured, gel-purified antigens (ELISA). Nevertheless, Fig. 4B clearly illustrates

amplification/broadening of the anti-Jo-1 response through serial assessment of antibody titers in individual mice immunized with MA/MBP. Conversely, the relative lack of cross recognition of murine Jo-1 following immunization with HA/MBP (even at 8 weeks) suggests that the response to human Jo-1 is uniphasic and does not uniformly extend beyond epitopes unique to human Jo-1 (compare lanes 1-5 in the two panels of Fig. 4A). As indicated in Fig. 4C, this overall pattern of antibody response is highly reproducible without evidence of strain dependence.

3.5. Induction of antigen-specific T cell responses

Based on the data supporting T cell dependence of this species-specific autoantibody production, we measured *in vitro* T cell responses to different versions of Jo-1 through CFSE labeling and flow cytometric assessment of dividing T cells. As shown in Fig. 5, T cells from mice primed with MA/MBP demonstrate preferential recognition of MA/MBP relative to HA/MBP or the MBP fusion partner.

3.6. Mice primed with murine Jo-1 develop muscle and lung inflammation

Inspection of muscle histopathology 8 weeks after immunization of B6.G7 mice shows sporadic foci of inflammatory cells in ~70% of the MA/MBP-immunized mice, but less commonly in mice immunized with HA/MBP (Fig. 6A; MA/MBP = 10/14 vs. HA/MBP = 4/9 vs. CFA alone 1/7). The infiltrative pattern is variable, with perimysial/epimysial inflammation in a perivascular distribution as well as endomysial inflammation and muscle fiber invasion/degeneration (Fig. 6A, panels a-c).

Even more striking than this muscle involvement is the degree and consistency of interstitial lung inflammation found in mice immunized with MA/MBP. The predominantly lymphocytic lung infiltrates tend to be perivascular and peribronchiolar, but also involve the alveoli (Fig. 6B). In B6.G7 mice, comparison of average histologic grade (0-4 scale defined in Section 2) shows a marked difference between MA/MBP (1.86) and HA/MBP (0.88) immunization (p 0.03, Mann-Whitney U-test), indicating that the observed histopathology is relatively specific for MA-induced immune activation against native epitopes not found in HA.

Further demonstrating the importance of self-directed anti-Jo-1 immune responses, NOD.*Idd3/5* mice immunized with MA/MBP also develop muscle and lung inflammation (Fig. 7). Unlike B6.G7 mice, however, NOD.*Idd3/5* mice require additional co-stimulation via OX40 to elicit significant muscle or lung pathology following MA/MBP immunization. As shown in other model systems, this dependence on co-stimulation reflects the enhancing effect of OX40 signaling on function and survival of antigen-specific effector/memory T cells [24].Beyond overall promotion of immune reactivity, OX40 co-stimulation obviates the relative species specificity of Jo-1-stimulated immune responses and leads to greater antibody cross-recognition of mouse Jo-1 in NOD.*Idd3/5* mice immunized with HA/MBP (Fig. 8). Corresponding to this augmented cross-recognition, the difference in muscle infiltration induced by MA/MBP versus HA/MBP immunization is not significant in NOD.*Idd3/5* mice (MA/MBP = 4/11 vs. HA/MBP = 4/10 vs. MBP = 0/8; Fig. 7A). Review of Fig. 7B shows that, in the context of OX40 co-stimulation, HA/MBP immunization also induces significant lung inflammation, with an average severity score of 1.7 (vs. MA/MBP = 1.82 vs. MBP = 0.75). The greater severity of lung inflammation in NOD.*Idd3/5* mice immunized with HA/MBP relative to B6.G7 mice receiving the same protein (NOD.*Idd3/5* = 1.7 vs. B6.G7 0.88) again correlates with markedly increased T cell and antibody cross recognition of murine Jo-1 following administration of the OX40 agonist antibody, OX86 (compare Fig. 8 with Fig. 4C).

4. Discussion

Taken together, these data demonstrate that immunization of both B6.G7 and NOD.*Idd3/5* mice with the amino terminal portion of mouse Jo-1 is capable of breaking/bypassing tolerance to this ubiquitous antigen. This breach of tolerance is very sequence specific in the absence of additional co-stimulation, occurring predominantly in response to MA that differs from HA by a mere 10 amino acids. Coupled with proliferation studies demonstrating the induction of T cells targeting murine Jo-1, the immunoprecipitation experiments and ELISA data showing epitope spreading (versus affinity maturation) following a single immunization with MA provide compelling evidence of an ongoing immune response fueled by murine Jo-1. Phenotypically, the immune response directed against self Jo-1 results in pronounced interstitial lung inflammation in a significant portion of MA/MBP-immunized animals, particularly when assessed 8 weeks following inoculation. Given the frequency and severity of lung inflammation compared to appropriate controls (see Figs. 6 and 7), this phenotype is not simply attributable to CFA (that has previously been linked to non-specific lung inflammation and granuloma formation [25,26]) or immune responses directed against the MBP fusion partner. Validating these conclusions, a previously published model of U1 snRNP-induced Mixed Connective Tissue Disease (MCTD) employing a similar immunization protocol with CFA emulsions of MBP fusion proteins demonstrated that 0/19 HLA-DR4 transgenic C57BL/6 mice receiving MBP alone developed significant lung infiltrates (compared to 11/24 mice immunized with U1 snRNP/MBP) [27].

In contrast to these histopathologic changes in lung tissue, muscle inflammation elicited by MA/MBP immunization is more sporadic and less prominent. Nevertheless, the triggering of muscle inflammation occurs most frequently with MA/MBP immunization (at least in B6.G7 mice), further highlighting the importance of directing the immune response against self/native Jo-1. In fact, the overall dependence of this system on immunization with murine versions of Jo-1 suggests that the failure of previous immunization strategies employing human Jo-1 to generate a defined phenotype stems from the inability to efficiently overcome/bypass tolerance to native Jo-1. Supporting this conclusion and the overall phenotypic correlation with anti-murine Jo-1 responses is the augmented level of muscle and lung inflammation seen in NOD.*Idd3/5* mice receiving the combination of HA/MBP and OX86, as these mice manifest significantly greater cross recognition of murine Jo-1 compared to mice not receiving additional OX40 co-stimulation (NOD.*Idd3/5* or B6.G7 mice immunized with HA/MBP alone, Fig. 4). Ultimately, although complete expression of the muscle phenotype may require additional stimuli such as induction of apoptosis and/or muscle regeneration to enhance presentation of target autoantigens [28], the concomitant development of interstitial lung disease in this model clearly mirrors that found in greater than 50% of patients with myositis and Jo-1 antibodies [29]. Moreover, the patchy/focal nature of muscle inflammation is characteristic of human disease in which the level of muscle dysfunction is often discordant with relatively mild histopathologic abnormalities. Hence, these results support a direct pathogenic connection between Jo-1-directed immune responses and the anti-synthetase syndrome in humans (which can occur in the absence of overt myositis).

Comparison of the immune responses to MA/MBP in B6.G7 and NOD.*Idd3/5* mice (which share the NOD I-A^{g7} MHC II locus but differ at non-MHC loci) does not yield any global differences that would implicate non-MHC loci in the development of interstitial lung pathology. However, the dependence on OX40 engagement in NOD.*Idd3/5* mice does highlight potentially significant epistatic interactions between B6-derived ICOS and CTLA-4 (encoded by genes within the *Idd5* locus) and co-stimulatory receptors/ligands that are of NOD origin. Beyond this differential requirement for co-stimulation, the phenotypic overlap between strains may appear surprising given the T_{H2} predominance of B6.G7 immune responses relative to NOD.*Idd3/5* and the impact of cytokine alteration on the expression of other autoimmune

phenomena such as diabetes. Yet, these findings are consistent with the occurrence of interstitial lung disease in humans with either DM or PM linked to Jo-1 antibody positivity; just as B6.G7 mice have different cytokine profiles and functional properties of T cell responses compared to NOD.*Idd3/5* mice [30,31], DM is thought to involve a significant T_{H2}-driven humoral component that contrasts with the predominant T_{H1} response found in PM [32]. Regardless of these potential mechanistic differences distinguishing the immune response(s) of NOD.*Idd3/5* and B6.G7 mice, the reproducibility of interstitial lung pathology and correlation with anti-*murine* Jo-1 reactivity in two independent strains further links the observed phenotype with MA-induced immune activation.

Interestingly, although the morphologic characteristics of lung inflammation are not significantly different between B6.G7 and NOD.*Idd3/5* mice, the pattern of muscle inflammation may segregate by genetic background. In these studies, for example, B6.G7 mice inoculated with MA predominantly manifest perimysial/perivascular infiltrates (analogous to DM) that appear distinct from the endomysial inflammation (paralleling the histopathology of PM) found in Jo-1-immunized NOD.*Idd3/5* mice. Clearly, however, delineating the exact role of non-MHC loci in this model will require larger follow-up studies with additional mice from both of these strains as well as congenic variants.

Attempting to elucidate the pathologic processes contributing to the phenotype of PM, investigators have previously developed a number of animal models employing viral infection, genetic manipulation, protein immunization, or DNA vaccination [33-35]. These paradigms of induced autoimmunity have complemented analysis of murine strains developing spontaneous forms of myositis, but none have fully replicated the immunologic phenotype of human disease or generated co-existing lung pathology found in the anti-synthetase syndrome. In the case of Jo-1, mice inoculated with a cDNA construct encoding a human version of this protein develop low titers of anti-Jo-1 antibody as well as cellular infiltrates causing myonecrosis (limited to injected muscle) [36]. On the other hand, these same mice do not manifest clinical or histologic evidence of muscle disease following immunization with *human* Jo-1 protein, consistent with our findings as well as those of other investigators. The discordant results of DNA and protein immunization point to several factors that may influence disease expression, including duration of antigen exposure as well as mode of antigen presentation [36]. Ultimately, however, neither method of immunization fully reproduces the PM phenotype, most likely because the resulting immune response is directed against human rather than native Jo-1.

Overall, the findings from our experimental approach provide a framework for the analysis of candidate autoantigens in myositis as well as other autoimmune diseases. While several models of antigen-induced autoimmunity have required co-immunization of foreign and self-versions of a particular protein [37,38], this system involves inoculation with murine Jo-1 alone. The ability to bypass tolerance (or overcome “clonal ignorance”) using only mouse Jo-1 indicates that potentially autoreactive B and T cells have escaped central tolerance and are immunologically “shielded” from target antigens under normal circumstances. Once exposed to the native immune system in the context of adjuvant, however, mouse Jo-1 is highly immunogenic with dominant B cell epitopes derived from conformational regions that are distinct from, rather than shared with, foreign (human) Jo-1. As shown by the peptide analysis in which identical amino acid sequences generate differential antibody responses against murine and human Jo-1 *protein*, the limited interspecies sequence variation significantly impacts the accessibility of structural motif(s) contributing to the overall immunogenicity of Jo-1—thus explaining the preferential B cell recognition of self epitopes that would not otherwise be predicted based on shared linear amino acid sequence.

Ultimately, defining the relative contribution of Jo-1-specific B and T cells in this system will hinge on future adoptive transfer strategies, particularly given emerging data on the function of B cells in the pathogenesis of diseases characterized by T cell-mediated tissue damage [39,40]. The latter approach will also permit assessment of the interaction between Jo-1-specific effector lymphocytes and regulatory T cells that have been shown to play a significant role in other models of antigen-driven auto-immunity [41,42]. Regardless of mechanism, the significance of the resulting tissue phenotype that includes pronounced lung inflammation extends beyond myositis and the anti-synthetase syndrome, as previously published models of interstitial lung disease (with the notable exception of U1 snRNP-induced MCTD [27,43]) have relied almost exclusively on chemical irritants for induction [44,45]. Refining the current system of Jo-1-triggered interstitial lung disease will therefore be critical in the study of pathologic processes ranging from connective tissue disease-associated lung inflammation to idiopathic pulmonary fibrosis.

Acknowledgements

We wish to thank Dr. Olivera Finn for critical review of this manuscript. This work was supported in part through a pilot and feasibility grant (DPA) awarded as a component of NIH RDCC grant AR047372.

Abbreviations

PM, polymyositis; DM, dermatomyositis; Jo-1, histidyl-tRNA synthetase; HA/MBP, amino terminal 151 amino acid fragment of human Jo-1 fused to MBP; MA/MBP, amino terminal 151 amino acid fragment of murine Jo-1 fused to MBP; MBP, maltose binding protein; CFA, complete Freund's adjuvant.

References

[1]. Yazici Y, Kagen LJ. Clinical presentation of the idiopathic inflammatory myopathies. Rheum Dis Clin N Am 2002;28:823–32.

[2]. Dalakas MC, Sivakumar K. The immunopathologic and inflammatory differences between dermatomyositis, polymyositis, and sporadic inclusion body myositis. Curr Opin Neurol 1996;9:235–9. [PubMed: 8839618]

[3]. Emslie-Smith AM, Engel AG. Microvascular changes in early and advanced dermatomyositis: a quantitative study. Ann Neurol 1990;27:343–56. [PubMed: 2353792]

[4]. Kissel JT, Mendell JR, Rammohan KW. Microvascular deposition of complement membrane attack complex in dermatomyositis. N Engl J Med 1986;314:329–34. [PubMed: 3945256]

[5]. Pignone A, Fiore G, Del Rosso A, Generini S, Matucci-Cerinic M. The pathogenesis of inflammatory muscle diseases: on the cutting edge among the environment, the genetic background, the immune response and the dysregulation of apoptosis. Autoimmun Rev 2002;1:226–32. [PubMed: 12849000]

[6]. Targoff IN. Humoral immunity in polymyositis/dermatomyositis. J Invest Dermatol 1993;100:116S–23. [PubMed: 8423380]

[7]. Yoshida S, Akizuki M, Mimori T, Yamagata H, Inada S, Homma M. The precipitating antibody to an acidic nuclear protein antigen, the Jo-1, in connective tissue diseases. Arthritis Rheum 1983;26:604–11. [PubMed: 6405755]

[8]. Miller FW, Twitty SA, Biswas T, Plotz PH. Origin and regulation of a disease-specific autoantibody response. Antigenic epitopes, spectrotype stability, and isotype restriction of anti-Jo-1 autoantibodies. J Clin Invest 1990;85:468–75. [PubMed: 1688885]

[9]. Stone K, Oddis CV, Fertig N, Katsumata Y, Lucas M, Vogt M. Anti-Jo-1 antibody levels correlate with disease activity in idiopathic inflammatory myopathy. Arthritis Rheum September 2007;56(9)

[10]. Miller FW, Waite KA, Biswas T, Plotz PH. The role of an autoantigen, histidyl-tRNA synthetase, in the induction and maintenance of autoimmunity. Proc Natl Acad Sci U S A 1990;87:9933–7. [PubMed: 1702223]

[11]. Raben N, Nichols R, Dohlman J, Mcphie P, Sridhar V, Hyde C, et al. A motif in human histidyl-tRNA synthetase which is shared among several aminoacyl-tRNA synthetases is a coiled-coil that is essential for enzymatic activity and contains the major autoantigenic epitope. JBC 1994;269:24277–83.

[12]. Martin A, Shulman MJ, Tsui FW. Epitope studies indicate that histidyl-tRNA synthetase is a stimulating antigen in idiopathic myositis. FASEB J 1995;9:1226–33. [PubMed: 7672516]

[13]. Craft J, Fatenejad S. Self antigens and epitope spreading in systemic autoimmunity. Arthritis Rheum 1997;40:1374–82. [PubMed: 9259415]

[14]. Ascherman DP, Oriss TB, Oddis CV, Wright TM. Critical requirement for professional APCs in eliciting T cell responses to novel fragments of histidyl-tRNA synthetase (Jo-1) in Jo-1 antibody-positive polymyositis. J Immunol 2002;169:7127–34. [PubMed: 12471150]

[15]. Mantegazza R, Andreetta F, Bernasconi P, Baggi F, Oksenberg JR, Simoncini O, et al. Analysis of T cell repertoire of muscle-infiltrating lymphocytes in polymyositis. J Clin Invest 1993;91:2880–6. [PubMed: 8514895]

[16]. O'Hanlon TP, Dalakas MC, Plotz PH, Miller FW. Predominant TCR-αβ variable and joining gene expression by muscle-infiltrating lymphocytes in the idiopathic inflammatory myopathies. J Immunol 1994;152:2569–76. [PubMed: 8133064]

[17]. Lapierre P, Beland K, Djilali-Saiah I, Alvarez F. Type 2 autoimmune hepatitis murine model: the influence of genetic background in disease development. J Autoimmun 2006;26:82–9. [PubMed: 16380229]

[18]. Ridgway WM, Fasso M, Lanctot A, Garvey C, Fathman CG. Breaking self-tolerance in nonobese diabetic mice. J Exp Med 1996;183:1657–62. [PubMed: 8666923]

[19]. Kanagawa O, Martin SM, Vaupel BA, Carrasco-Marin E, Unanue ER. Autoreactivity of T cells from nonobese diabetic mice: an I-Ag7-dependent reaction. Proc Natl Acad Sci U S A 1998;95:1721–4. [PubMed: 9465083]

[20]. Elliott JF, Liu J, Yuan Z, Bautista-Lopez N, Wallbank SL, Suzuki K, et al. Autoimmune cardiomyopathy and heart block develop spontaneously in HLA-DQ8 transgenic IAbeta knockout NOD mice. Proc Natl Acad Sci U S A 2003;100:13447–52. [PubMed: 14570980]

[21]. Salomon B, Rhee L, Bour-Jordan H, Hsin H, Montag A, Soliven B, et al. Development of spontaneous autoimmune peripheral polyneuropathy in B7-2-deficient NOD mice. J Exp Med 2001;194:677–84. [PubMed: 11535635]

[22]. Bernard NF, Ertug F, Margolese H. High incidence of thyroiditis and anti-thyroid autoantibodies in NOD mice. Diabetes 1992;41:40–6. [PubMed: 1727738]

[23]. Goillot E, Mutin M, Touraine JL. Sialadenitis in nonobese diabetic mice: transfer into syngeneic healthy neonates by splenic T lymphocytes. Clin Immunol Immunopathol 1991;59:462–73. [PubMed: 2029797]

[24]. Gramaglia I, Jember A, Pippig S, Weinberg AD, Killen N, Croft M. The OX40 costimulatory receptor determines the development of CD4 memory by regulating primary clonal expansion. J Immunol 2000;165:3043–50. [PubMed: 10975814]

[25]. Howell C, Yoder TD. Murine experimental autoimmune hepatitis: non-specific inflammation due to adjuvant oil. Clin Immunol Immunopathol 1994;72:76–82. [PubMed: 8020196]

[26]. Broderson JR. A retrospective review of lesions associated with the use of Freund's adjuvant. Lab Anim Sci 1989;39:400–5. [PubMed: 2811278]

[27]. Greidinger EL, Zang Y, Jaimes K, Hogenmiller S, Nassiri M, Bejarmo P, et al. A murine model of Mixed Connective Tissue Disease induced with U1 small nuclear RNP antigen. Arthritis Rheum 2006;54:661–9. [PubMed: 16453294]

[28]. Casciola-Rosen L, Nagaraju K, Plotz P, Wang K, Levine S, Gabrielson E, et al. Enhanced autoantigen expression in regenerating muscle cells in idiopathic inflammatory myopathy. J Exp Med 2005;201:591–601. [PubMed: 15728237]

[29]. Hochberg MC, Feldman D, Stevens MB, Arnett FC, Reichlin M. Antibody to Jo-1 in polymyositis/dermatomyositis: association with interstitial pulmonary disease. J Rheumatol 1984;11:663–5. [PubMed: 6334746]

[30]. Koarada S, Wu Y, Ridgway WM. Increased entry into the IFN-gamma effector pathway by CD4 + T cells selected by I-Ag7 on a nonobese diabetic versus C57BL/6 genetic background. J Immunol 2001;167:1693–702. [PubMed: 11466393]

[31]. Koarada S, Wu Y, Olshansky G, Ridgway WM. Increased nonobese diabetic Th1:Th2 (IFN-gamma:IL-4) ratio is CD4 + T cell intrinsic and independent of APC genetic background. J Immunol 2002;169:6580–7. [PubMed: 12444170]

[32]. Aleksza M, Szegedl A, Antal-Szalmas P, Irinyi B, Gergely L, Ponyi A, et al. Altered cytokine expression of peripheral blood lymphocytes in polymyositis and dermatomyositis. Ann Rheum Dis 2005;64:1485–9. [PubMed: 15829578]

[33]. Nagaraju K, Plotz P. Animal models of myositis. Rheum Dis Clin North Am 2002;28:917–33. [PubMed: 12506778]

[34]. Sugihara T, Sekine C, Nakae T, Kohyama K, Harigai M, Iwakura Y, et al. A new murine model to define the critical pathologic and therapeutic mediators of polymyositis. Arthritis Rheum 2007;56:1304–14. [PubMed: 17394136]

[35]. Katsumata Y, Harigai M, Sugiura T, Kawamoto K, Kawaguchi Y, Matsumoto Y, et al. Attenuation of Experimental Autoimmune Myositis by blocking Inducible Costimulator (ICOS)-ICOS-ligand interaction. J Immunol September 15 2007;179(6)

[36]. Blechynden LM, Lawson MM, Tabarias H, Garlepp MJ, Sherman J, Raben N, et al. Myositis induced by naked DNA immunization with the gene for histidyl-tRNA synthetase. Hum Gene Ther 1997;8:1469–80. [PubMed: 9287147]

[37]. Mamula M, Lin R-H, Janeway C, Hardin J. Breaking T cell tolerance with foreign and self co-immunogens. J Immunol 1992;149:789–95. [PubMed: 1321851]

[38]. Jones D, Palmer J, Bennett K, Robe AJ, Yeaman SJ, Robertson H, et al. Investigation of a mechanism for accelerated breakdown of immune tolerance to the primary biliary cirrhosis-associated autoantigen, pyruvate dehydrogenase complex. Lab Invest 2002;82:211–9. [PubMed: 11850534]

[39]. Youinou P. B cell conducts the lymphocyte orchestra. J Autoimmun 2007;28:143–51. [PubMed: 17363215]

[40]. Lou Y-H, Borillo J. Migration of T cells from nearby inflammatory foci into antibody bound tissue: a relay of T cell and antibody actions in targeting native autoantigen. J Autoimmun 2003;21:27–35. [PubMed: 12892733]

[41]. Abbas AK, Lohr J, Knoechel B. Balancing autoaggressive and protective T cell responses. J Autoimmun 2007;28:59–61. [PubMed: 17363216]

[42]. Sharma R, Jarjour WN, Zheng L, Gaskin F, Man Fu S, Ju S-T. Large functional repertoire of regulatory T-cell suppressible autoimmune T cells in scurfy mice. J Autoimmun 2007;29:10–9. [PubMed: 17521882]

[43]. Keith MP, Moratz C, Tsokos GC. Anti-RNP immunity: Implications for tissue injury and the pathogenesis of connective tissue disease. Autoimmun Rev 2007;6:232–6. [PubMed: 17317614]

[44]. Bozelka BE, Sestini P, Gaumer HR, Hammad Y, Heather CJ, Salvaggio JE. A murine model of asbestosis. Am J Pathol 1983;112:326–37. [PubMed: 6311019]

[45]. Haston CK, Wang M, Dejournett RE, Zhou X, Ni D, Gu X, et al. Bleomycin hydrolase and a genetic locus within the MHC affect risk for pulmonary fibrosis in mice. Hum Mol Genet 2002;11:1855–63. [PubMed: 12140188]

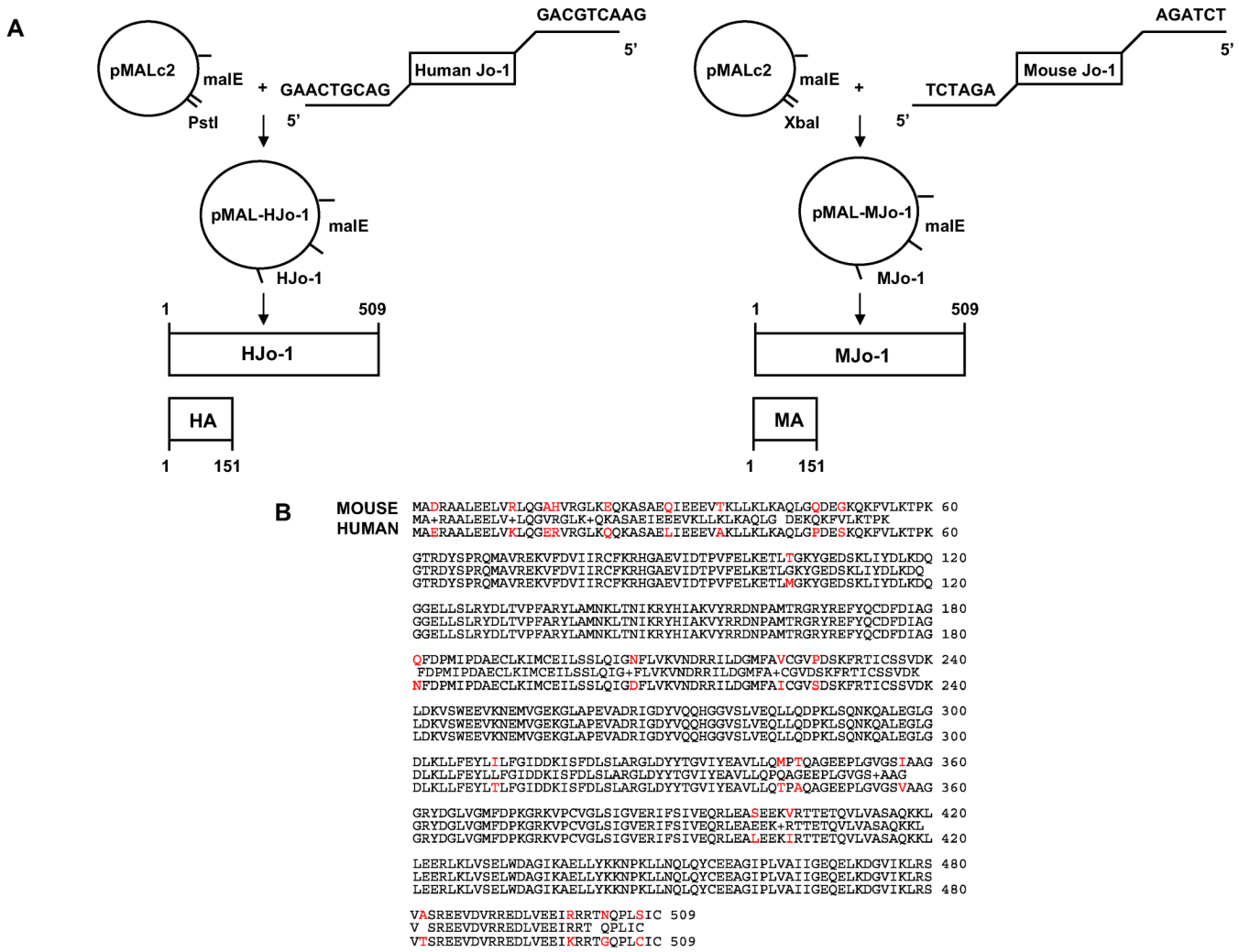

Fig. 1.

Cloning of human and murine histidyl-tRNA synthetase (Jo-1). (A) Full length sequences encoding human or murine Jo-1 were amplified from cDNA via PCR using primers containing terminal restriction enzyme recognition sequences as indicated. Following restriction enzyme digestion of these inserts, the Jo-1 sequences were inserted into the bacterial Maltose Binding Protein expression vector pMALc2. Automated sequencing was performed to confirm proper orientation and to rule out errors introduced during PCR amplification. (B) Amino acid sequence alignment comparing murine and human Jo-1. Sequence differences are highlighted in red.

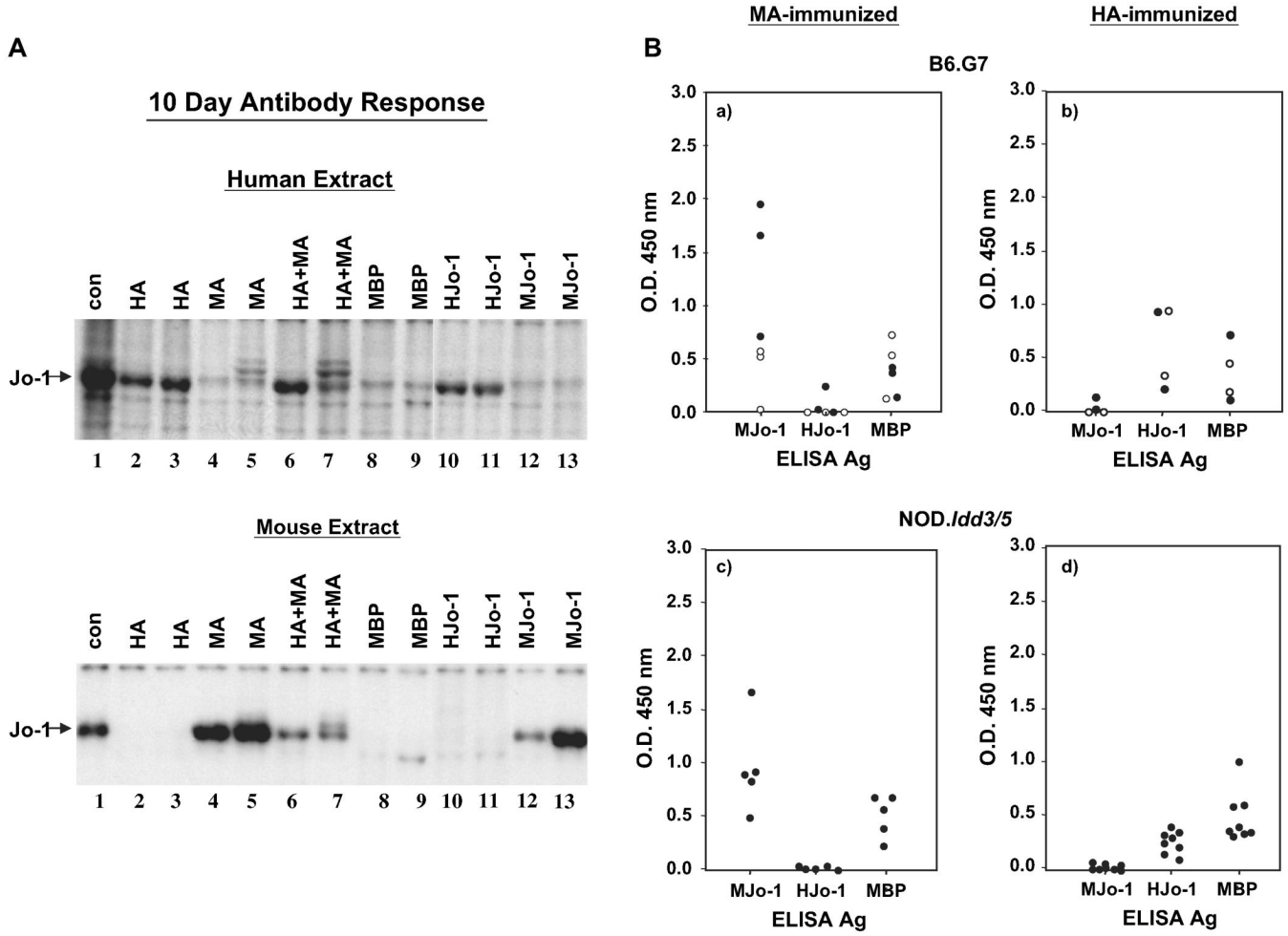

Fig. 2.

Short term antibody responses to Jo-1 immunization are driven by species-specific epitopes. (A) Immunoprecipitation of ^{35}S-methionine-labeled human K562 cell extract (top panel) or a murine cell extract (lower panel) with serum obtained 10 days following immunization of mice with indicated Jo-1 proteins yields a ~50 kDa protein (Jo-1) designated by the arrow. Strains tested include C57BL/6 and B6.G7. Con = anti-Jo-1 human reference serum, MBP = Maltose Binding Protein, MJo-1 = full length mouse Jo-1, HJo-1 = full length human Jo-1, MA = amino acids 1-151 of mouse Jo-1 fused to MBP, and HA = amino acids 1-151 of human Jo-1 fused to MBP. (B) Sera obtained 10 days following immunization of B6.G7 (a, b) or NOD.*Idd3/5* (c, d) mice with the indicated antigens were subjected to ELISA as described in Section 2. Scatter plots depict mean OD_{450} readings of anti-murine or anti-human Jo-1 antibody levels using serum dilutions of 1:5000 and antigen concentrations of 0.1 μg/ml. Closed circles represent mice immunized with MA/MBP (a, c) or HA/MBP (b, d), while open circles correspond to mice immunized with full-length MJo-1 (a) or HJo-1 (b).

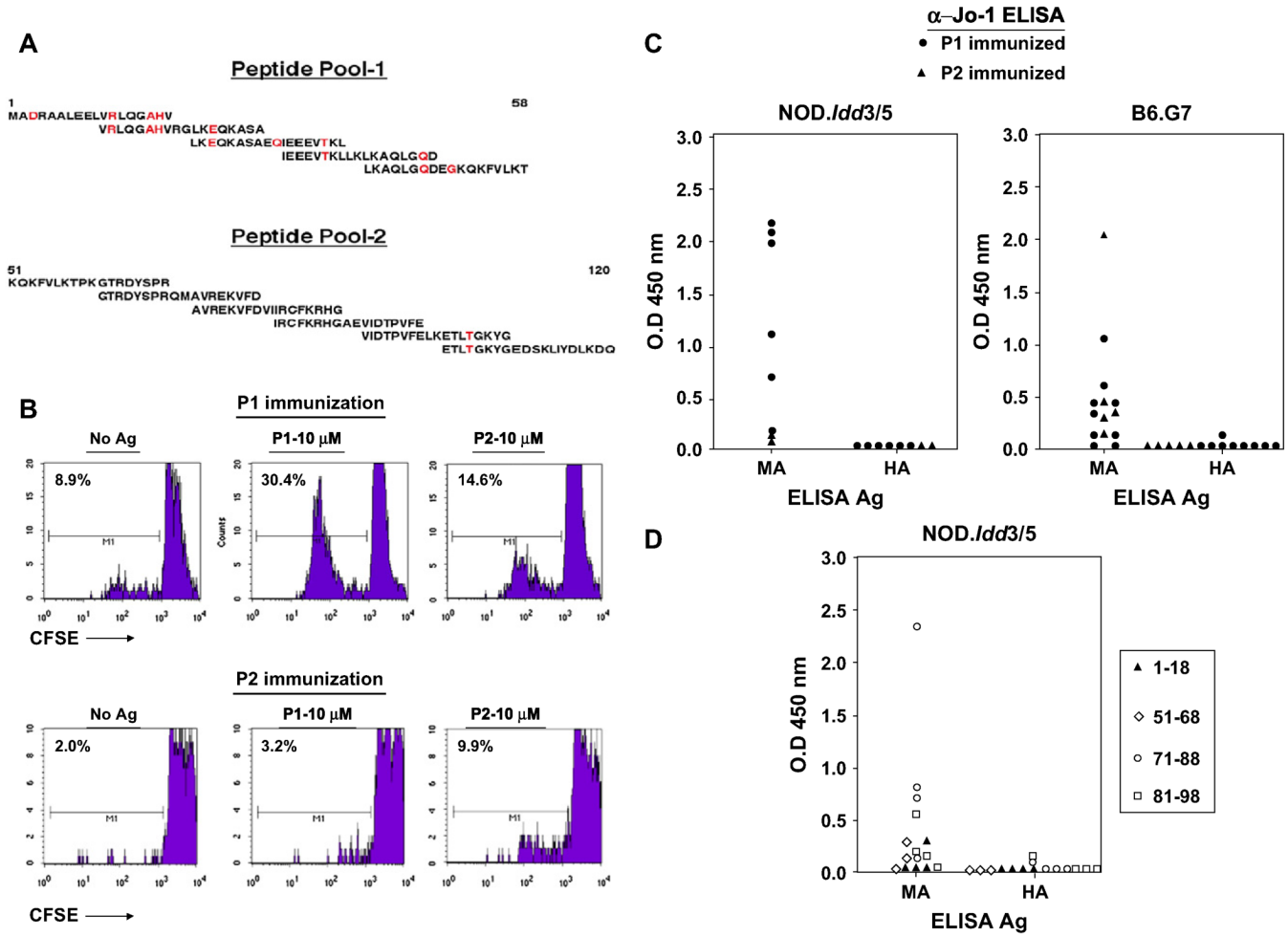

Fig. 3.

Immunization with purified mouse Jo-1 peptides is sufficient to bypass B and T cell tolerance. NOD.*Idd3/5* and B6.G7 mice were subcutaneously immunized with different mixtures of murine Jo-1-derived peptides (100 μg of OX86 co-administered intraperitoneally on Days 0 and 2 in NOD.*Idd3/5* mice) and then sacrificed on Day 14-24. While panel A illustrates the overlapping sequences of these peptides (Peptide Pool 1 = P1 and Peptide Pool 2 = P2; red highlighting indicates amino acids distinguishing murine and human Jo-1 sequences), panel B shows representative 96 h proliferative responses of CFSE labeled NOD.*Idd3/5* splenocytes following secondary *in vitro* challenge with the same peptide pools. Panel C depicts anti-Jo-1 IgG levels (measured by ELISA) of serum samples obtained 14-24 days following immunization of NOD.*Idd3/5* or B6.G7 mice with mouse Jo-1 peptide pools as outlined in Section 2. Antibody responses to immunization with selected peptides comprising peptide pools 1 (closed triangles) and 2 (open figures) are shown in panel D. Values for individual mice represent the mean OD_{450} readings of triplicate samples (minus background anti-MBP IgG level). Control sera demonstrated equivalent binding of the substrate antigens MA = MA/MBP and HA = HA/MBP (not shown).

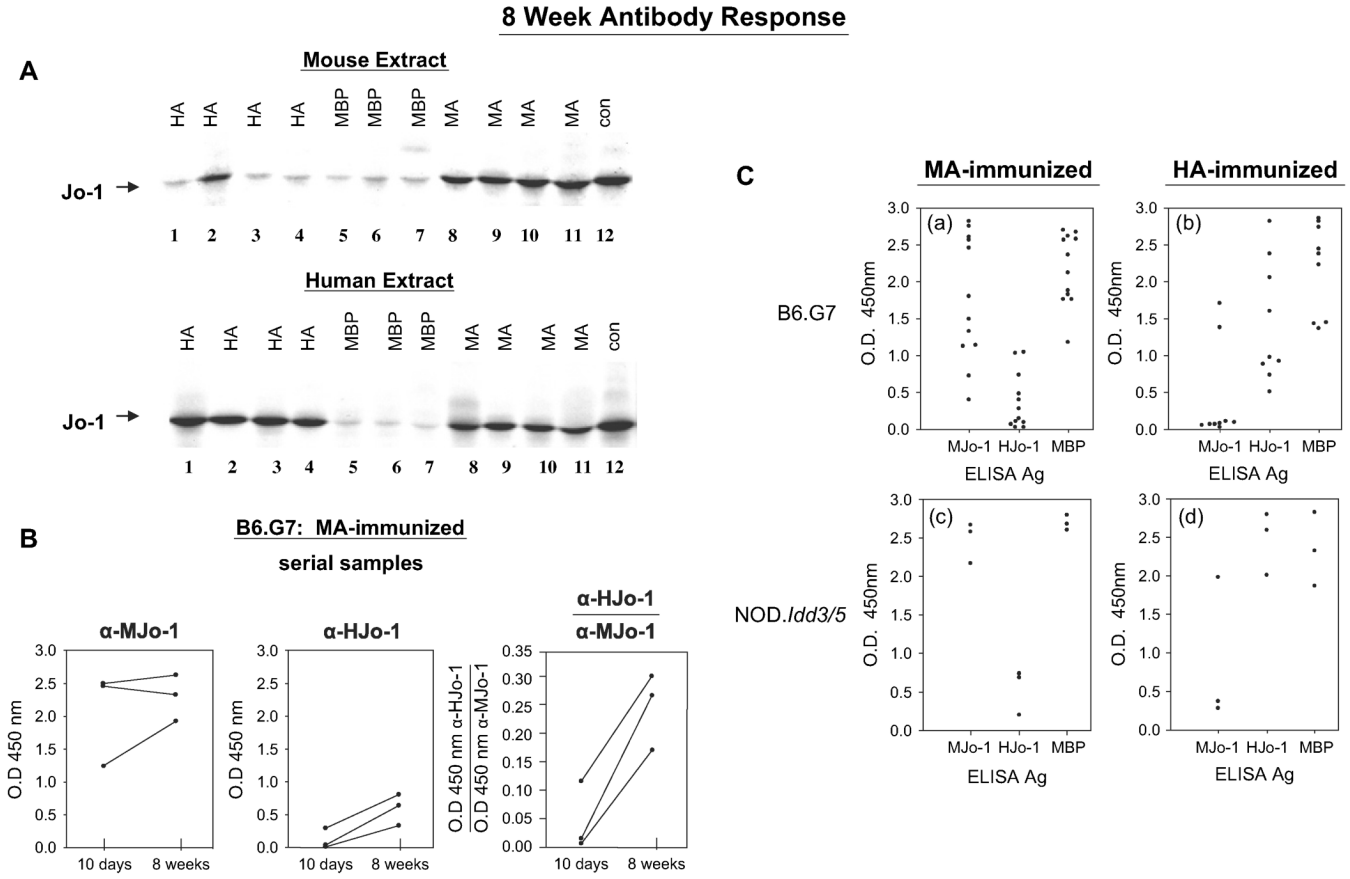

Fig. 4.

Preferential development of cross-reactive autoantibodies occurs by 8 weeks in mice receiving murine Jo-1 fragment A (MA). (A) Immunoprecipitation of ^{35}S-methionine-labeled extracts derived from murine cells (top panel) or the human cell line K562 (lower panel) were performed with serum samples obtained 8 weeks following immunization. A control human reference serum showing cross-reactivity to mouse Jo-1 (lane 12) is shown for comparison. Protein abbreviations are identical to those used in Fig. 2. (B) Serial anti-murine and anti-human Jo-1 antibody titers were assessed via ELISA 10-56 days following MA immunization of B6.G7 mice using full length human or murine Jo-1 as substrate antigens. In the third panel, values expressed on the y axis represent ratios of anti-human Jo-1 OD_{450}: anti-murine Jo-1 OD_{450}. ELISA quantification of anti-murine and anti-human Jo-1 antibody responses 8 weeks following immunization shows greater diversification following immunization with MA (C). Dots represent mean OD_{450} values for antibody titers from individual mice immunized with MA (a, c) or HA (b, d).

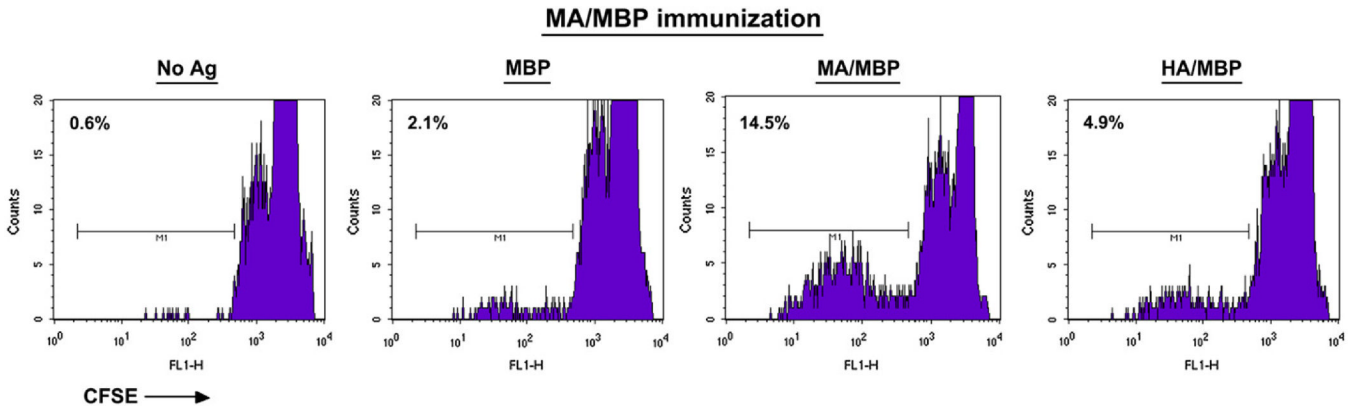

Fig. 5.

Splenic T cells from murine Jo-1-immunized mice proliferate following secondary *in vitro* challenge with MA. Eight weeks following immunization of B6.G7 mice with the amino terminal fragment of mouse Jo-1 (MA/MBP), splenocytes were CFSE labeled and combined with the indicated antigens for 4 days prior to harvesting and cell surface staining with anti-CD4 antibodies. Histograms depict the reduction in CFSE-induced fluorescence of CD4 + T cells.

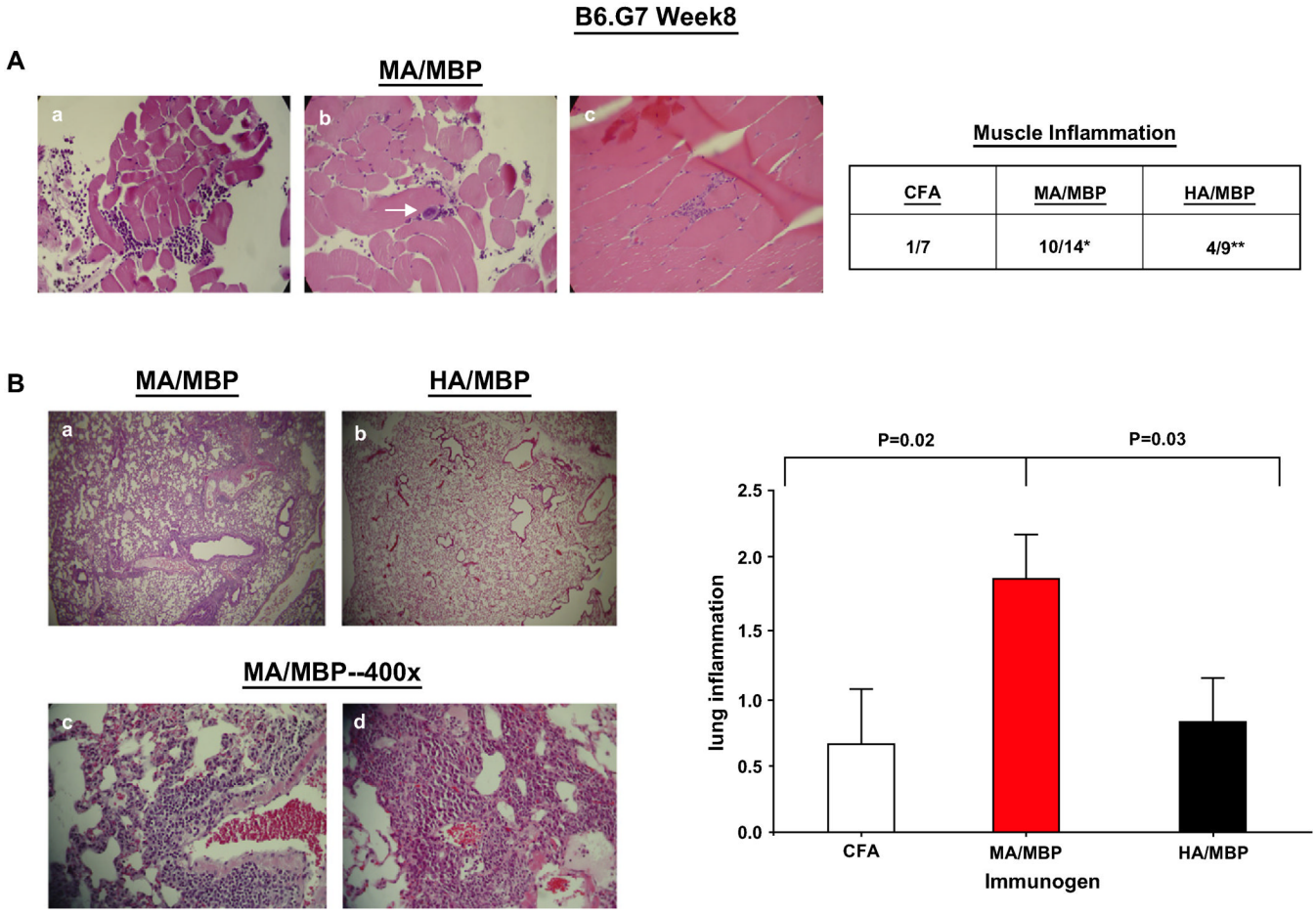

Fig. 6.

Immunization with murine Jo-1 induces muscle and lung inflammation in B6.G7 mice. (A) Representative H&E stained quadriceps/hamstring muscle sections at 400× magnification from B6.G7 mice sacrificed 8 weeks following immunization with emulsions of MA/MBP (amino acids 1-151 of mouse Jo-1 fused to MBP) in CFA. While panels a-b demonstrate epimysial/perimysial inflammation and perivascular accumulation of lymphocytes (arrow, panel b), panel c shows an endomysial infiltrate. The accompanying table reflects the frequency of muscle inflammation following immunization with MA/MBP, HA/MBP, or CFA alone (*p = 0.02, MA/MBP vs. CFA; **p = 0.31, HA/MBP vs. CFA-Fisher's exact test). (B) Panels a-d illustrate H&E stained lung sections of B6.G7 mice 8 (panels a-c) or 16 (d) weeks following immunization with Jo-1 proteins. Panels a and b compare representative areas of lung (50×) from mice immunized with MA/MBP (panel a) or HA/MBP (panel b). Panels c-d depict 400× power magnification of dense infiltrates surrounding large airways, branches of the pulmonary artery, and smaller blood vessels in lung tissue obtained from MA/MBP-immunized mice. The bar graph reflects the severity of Jo-1-induced lung inflammation 8 weeks after immunization of B6.G7 mice with different versions of Jo-1. Numerical values on the y axis indicate scoring confirmed by a blinded pathologist according to the criteria outlined in Section 2 (error bars reflect S.E.M.), while immunizing proteins are indicated along the x-axis (abbreviations as previously defined). The p-value reflects statistical comparison (using the Mann-Whitney U-test) of different immunized groups that include all mice from multiple experiments ($n_{MA/MBP}$ 14, $n_{HA/MBP}$ = 9, n_{CFA} = 7).

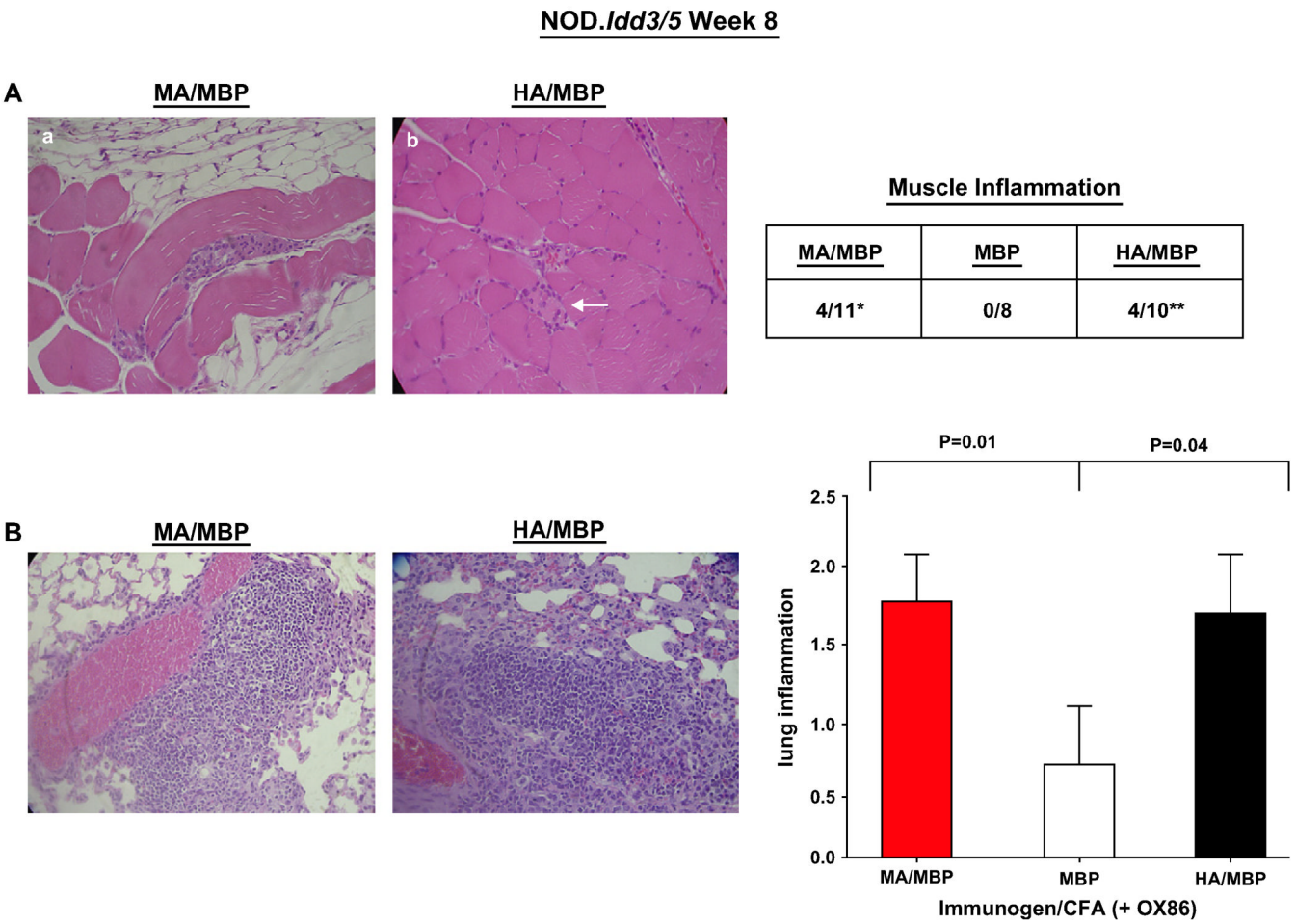

Fig. 7.

NOD.*Idd3/5* mice immunized with murine or human Jo-1 develop muscle inflammation and interstitial lung disease. (A) Representative muscle sections from NOD.*Idd3/5* mice immunized with CFA emulsions of MA/MBP (panel a) or HA/MBP (panel b) demonstrate muscle fiber invasion/degeneration and endomysial inflammation (arrow, panel b). The table summarizes the frequency of muscle inflammation induced by MA/MBP or HA/MBP immunization in comparison to MBP inoculation (*$p = 0.10$, MA/MBP vs. MBP; **$p = 0.09$, HA/MBP vs. MBP—Fisher's exact test). (B) Micrographs and grading of lung inflammation 8 weeks following immunization of NOD.*Idd3/5* mice. Co-administration of the OX40 agonist antibody OX86 is indicated along with the immunogen on the x-axis of the associated bar graph. Statistical comparison of lung severity scores incorporates all data from at least two independent experiments per cohort ($n_{MA/MBP} = 11$, $n_{HA/MBP} = 10$, $n_{MBP} = 8$) and is again based on the Mann-Whitney *U*-test.

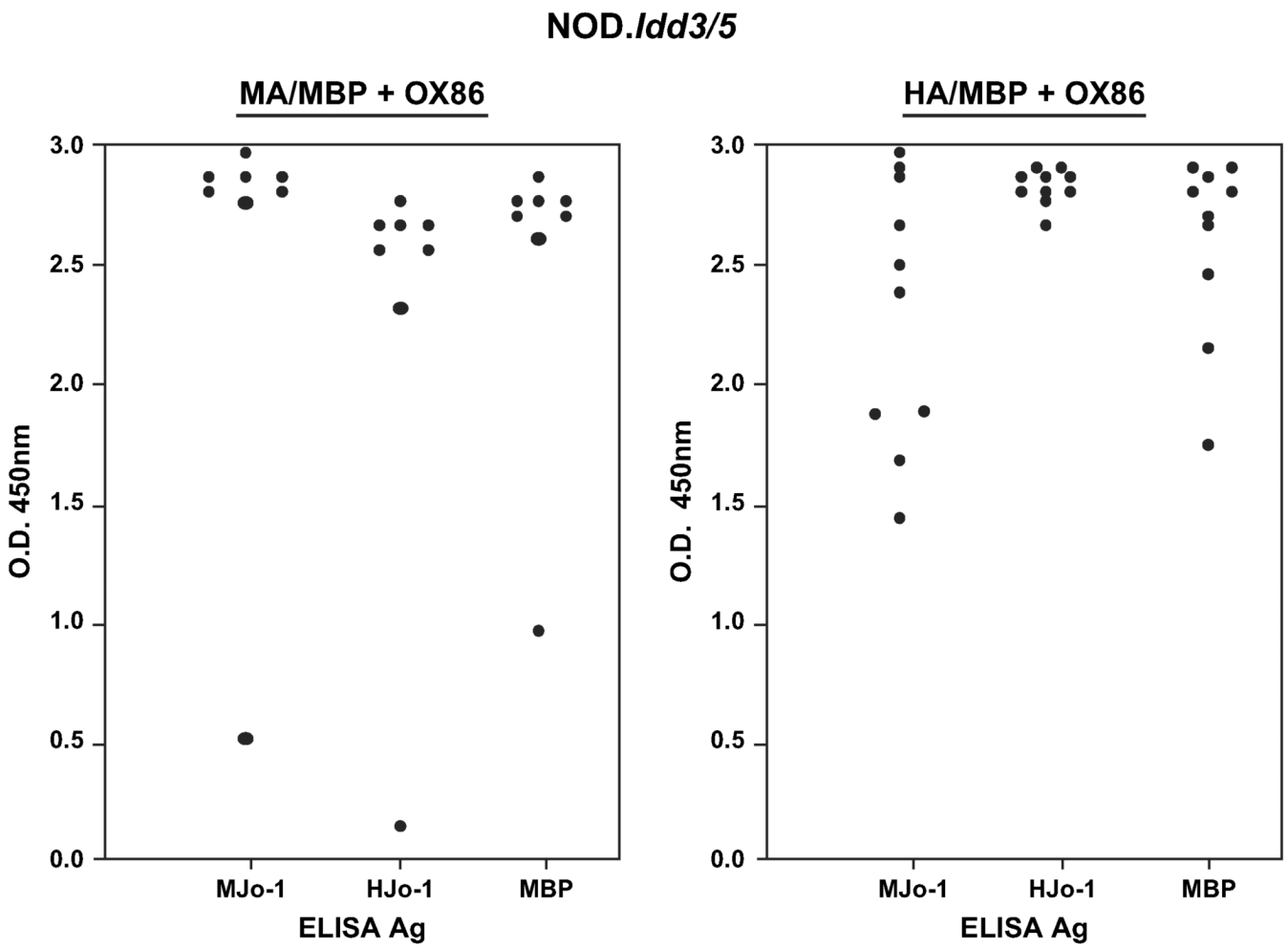

Fig. 8.

OX40 co-stimulation promotes antibody cross recognition of murine and human Jo-1. The ELISA values show comparative antibody titers in NOD.*Idd3/5* mice 8 weeks following subcutaneous protein immunization and co-administration of the OX40 agonist antibody OX86. Serum dilutions and substrate antigen concentrations are identical to those outlined in the legend to Fig. 4.